LBL--18240-Rev.

DE85 007471

STUDY OF TRANSFER AND BREAKUP REACTIONS WITH THE PLASTIC BOX*

R. G. Stokstad[a], C. R. Albiston[a], M. Bantel[a], Y. Chan[a], P. J. Countryman[b], S. Gazes[a], B. G. Harvey[a], H. Homeyer[c], M. J. Murphy[a], I. Tserruya[a], K. Van Bibber[b], and S. Wald[a]

a) Nuclear Science Division
University of California
Lawrence Berkeley Laboratory
Berkeley, CA 94720

b) Department of Physics
Stanford University
Stanford, CA 94305

c) Hahn-Meitner Institute
Berlin, Federal Republic of Germany.

Invited talk presented by R. G. Stokstad at the International Conference on Nuclear Physics, Bhabha Atomic Research Centre, Bombay, India, December 27-31, 1984. Proceedings to be published.

*This work was supported by the Director, Office of Energy Research, Division of Nuclear Physics of the Office of High Energy and Nuclear Physics, and by the Nuclear Sciences of Basic Energy Sciences Program of the U.S. Department of Energy under Contracts DE-AC03-76SF00098 and DE-AM03-76SF00326.

Abstract

The study of transfer reactions with heavy-ion projectiles is complicated by the frequent presence of three or more nuclei in the final state. One prolific source of three-body reactions is the production of a primary ejectile in an excited state above a particle threshold. A subset of transfer reactions, viz., those producing ejectiles in bound states, can be identified experimentally. This has been accomplished with a 4π detector constructed of one-millimeter-thick scintillator paddles of dimension 20 cm x 20 cm. The paddles are arranged in the form of a cube centered around the target with small entrance and exit apertures for the beam and the projectile-like fragments, (PLF). The detection of a light particle (e.g., a proton or an alpha particle) in coincidence with a PLF indicates a breakup reaction. The absence of any such coincidence indicates a reaction in which all the charge lost by the projectile was transferred to the target. With this technique we have studied the transfer and breakup reactions induced by 220 and 341 MeV ^{20}Ne ions on a gold target. Ejectiles from Li to Ne have been measured at several scattering angles. The absolute cross sections, angular distributions and energy spectra for the transfer and breakup reactions are presented. Relatively large cross sections are observed for the complete transfer of up to seven units of charge (i.e., a nitrogen nucleus). The relatively large probabilities for ejectiles to be produced in particle-bound states suggest that on the average, most of the excitation energy in a collision resides in the heavy fragment when mass is transferred from the lighter to the heavier fragment. The gross features and trends in the energy spectra for transfer and breakup reactions are similar.

I. Introduction.

Heavy-ion reactions at bombarding energies from only a few MeV per nucleon above the barrier to the highest energies yet studied (~ 2 GeV/u) all exhibit a quasi-elastic peak. This peak consists of nuclei at forward or grazing angles with masses close to or smaller than the projectile mass and moving with approximately the beam velocity. While these products, when observed inclusively, exhibit some similarities at all energies[1], the underlying reaction mechanisms are expected to be quite different at low and at very high bombarding energies. In the former case the transfer of nucleons from projectile to target yielding a two-body final state is predominant, whereas in the latter case the very high velocity of the projectile nucleons prevents their being captured by the target, even though the target might shear many nucleons from the projectile. Another mechanism that can produce a three-body (or more) final state containing a quasi-elastic fragment is the sequential decay of an excited projectile-like nucleus. Since the nucleus need have only ~ 10 MeV of excitation to be above threshold for particle decay, this process can occur in principle at all but the very lowest bombarding energies. The intermediate bombarding energy region, 10-100 MeV/nucleon, is possibly host to all three mechanisms: transfer, sequential decay, and fragmentation.

It is thus important to design experiments that enable the separation of the various reaction mechanisms or, at least, that identify one particular component. Coincidence experiments address this problem and there have been many of these done at the lower bombarding energies, though relatively few at higher energies. Characteristic γ rays[2] or x-rays[3] emitted by the target-like fragment can identify transfer reactions; the number of neutrons emitted by the excited heavy partner can help separate transfer and breakup,[4] and high resolution two-particle coincidence experiments are able to demonstrate sequential decay[5]. A streamer chamber[6], triggered by a projectile-like fragment (PLF), is able to detect the presence of any additional light charged particles and can effectively distinguish two-body from multibody reactions. The device described here, the "plastic box", is modeled after the streamer chamber in that it records the presence or absence of additional charged particles accompanying the PLF. It is a "4π detector" and can tell us whetner a particular projectile fragment is one member of a two-body reaction. Unlike the streamer chamber, it is able to acquire data at relatively high rates and does not entail scanning a photograph of each event. It has been designed for use at intermediate energies.

The plastic box singles out the class of reactions in which charge is

removed from the projectile, transferred to and captured by the target, and in which the emerging primary PLF is in a bound state. Operationally we refer to this class of events as transfer reactions. This class includes those cases in which the excited target-like fragment (TLF) subsequently decays by neutron emission, fission, or light-particle evaporation. Three-body reactions in which a fast light charged particle is emitted at forward angles along with the PLF will be referred to collectively as breakup reactions. This operational definition includes sequential decay of the primary excited PLF as well as all preequilibrium processes producing fast charged particles.

II. The detector system.

The plastic box is an array of plastic scintillator paddles, light guides and phototubes arranged around the target in the fashion shown schematically in Fig. 1. The light guides and phototubes are shown only for the top wall (wall 5) of the cube. Each wall consists of two separate scintillator paddles made of NE102A, each 20 cm high, 20 cm wide, and 1 mm thick. The beam and the projectile-like fragments emerge through a slot in wall 1. Two movable telescopes, each having three solid-state elements, can cover the angular range from ~ 5^{0} to ~ 21^{0}. Additional scintillator paddles (not shown)

The Plastic Box –
A 4π Detector for Charged Particles

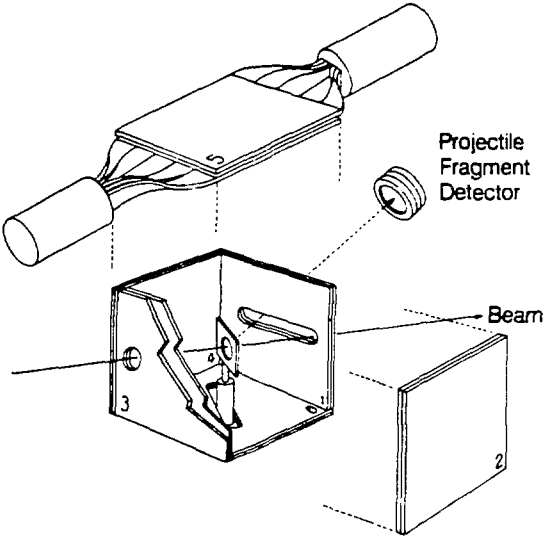

Fig. 1. Schematic diagram of the plastic box.

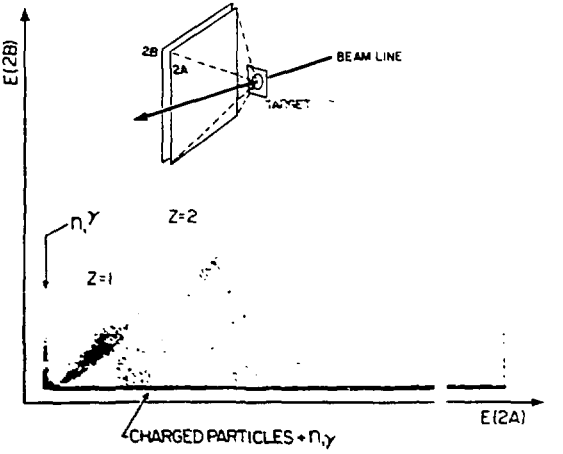

Fig. 2. A two-dimensional singles spectrum of the light output from the inner (A) and outer (B) paddles of the wall. Events appearing on the vertical axis ($\bar{A}B$) can only be due to neutral particles.

are located behind the telescopes and downstream close to 0^0 in order to detect most of the light particles that escape through the slot in wall 1. Each of the twelve phototubes on the cube plus the four on the additional paddles is serviced by a charge-sensitive ADC. All signals are handled by a CAMAC system.

The response of a wall to various particles is illustrated in Fig. 2. The light output from the inner paddle (A) and outer paddle (B) can be used to identify neutral particles and to give some measure of identification for charged particles sufficiently energetic to penetrate the inner paddle. The type of event with a signal in paddle B and none in paddle A, denoted by ($\overline{A}B$), is a direct measure of the system's efficiency for detection of neutral particles. The paddles were made thin to minimize the efficiency for neutrals and chosen to be identical so that the number of those events ($\overline{A}\overline{B}$) due to neutral particles is determined directly. Studies have been made of the procedures for (i) determining the energy thresholds for charged particle detection and (ii) correcting for neutral particles. A comparison was made of results obtained with the plastic box for the reaction ^{16}O + Sn with results for ^{16}O + CsI from the streamer chamber, as a check on the whole technique. More information on the detection system is available in Ref. 7.

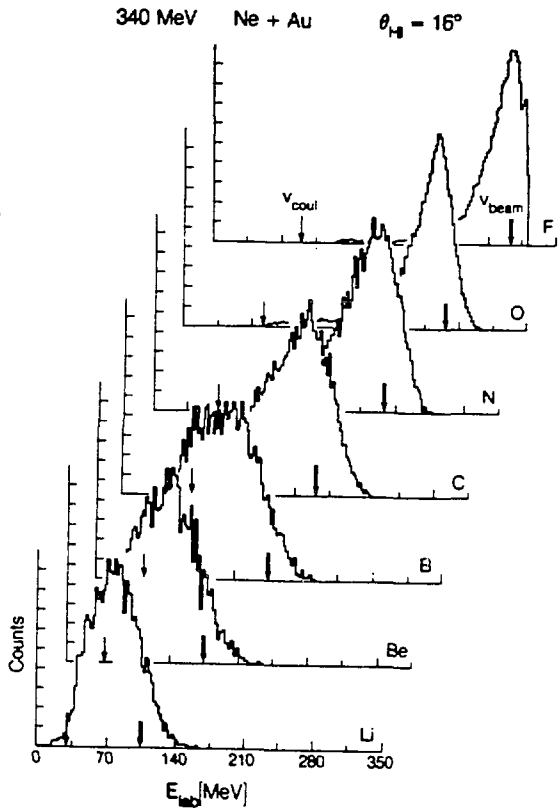

Fig. 3. Inclusive energy spectra for ejectiles near the grazing angle illustrate the quasi-elastic nature of the reaction products.

III. Choice of the Ne + Au reaction.

A number of factors influenced our choice of the projectile and target. A heavy target was desirable because neutron emission and fission are the favored modes of decay and the evaporation of charged particles is

suppressed. The latter, in contrast to neutrons and fission fragments, would be detected by the scintillators. The projectile should be a "light" heavy ion because higher velocities for these are available from the cyclotron, and because the resolution of adjacent masses is still possible with a solid-state telescope. The ^{20}Ne + Au system satisfied these criteria and had the additional advantage that studies of the inclusive reactions had already been done at several energies at the Hahn-Meitner Institute.[8]

Measurements with the plastic box were made at Ne bombarding energies of 220 and 341 MeV, i.e., at 11 and 17 MeV per nucleon. The quasi-elastic peak is pronounced for all elements from fluorine down to lithium, as shown by the inclusive spectra in Fig. 3. These spectra were taken at an angle close to the grazing angle for 17 MeV/u ^{20}Ne + Au. The arrows labeled v_{beam} and v_{coul} denote, respectively, the energies corresponding to the beam velocity and the Coulomb repulsion energy. Kinematic models assuming linear and angular momentum matching for incoming and outgoing orbits reproduce the most probable velocities.[9] The inclusive features of this reaction thus suggest that we are dealing with quasi-elastic (as opposed to deep-inelastic) reactions. The subject to be addressed by the plastic box concerns the mechanisms producing these fragments - how much is due to transfer, and how much to breakup.

IV. Experimental results.

A. Yields

It is easiest to obtain an overview of the experimental results when individual isotopes are summed and elemental yields are considered. The telescopes did resolve the isotopes of the PLF's (at 341 MeV) and, therefore, most of the results presented below are also available by isotope as well as by element.

The first question to ask about any fragment observed in the particle telescope is how many of the six walls observed an associated charged particle. This number is denoted by S. The most straightforward case to interpret is S = 0, i.e., no additional charged particles were observed. This implies that all the charge removed from the projectile must have been captured by the target and that the PLF was left in a bound state. Furthermore, the TLF must have emitted no light charged particle. The probability that a PLF of charge Z corresponded to S = 0, or to a larger value of S (corrected for random coincidences) is given in Fig. 4 for 220 MeV

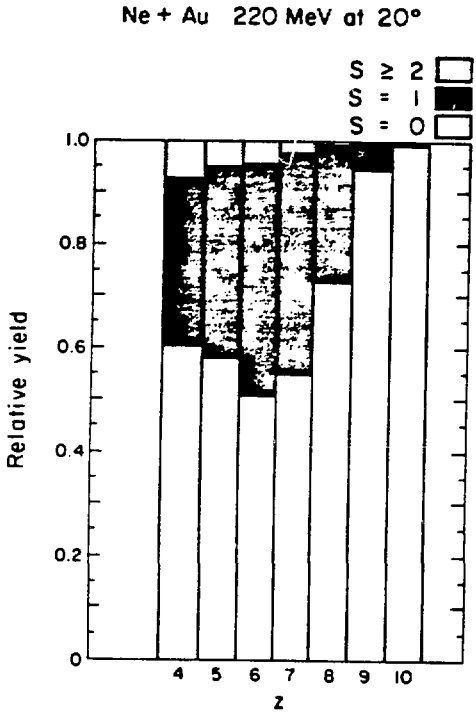

Fig. 4. The relative yield of ejectiles having none, one, or more than one scintillator walls in coincidence for an ejectile of charge Z, at a bombarding energy of 220 MeV.

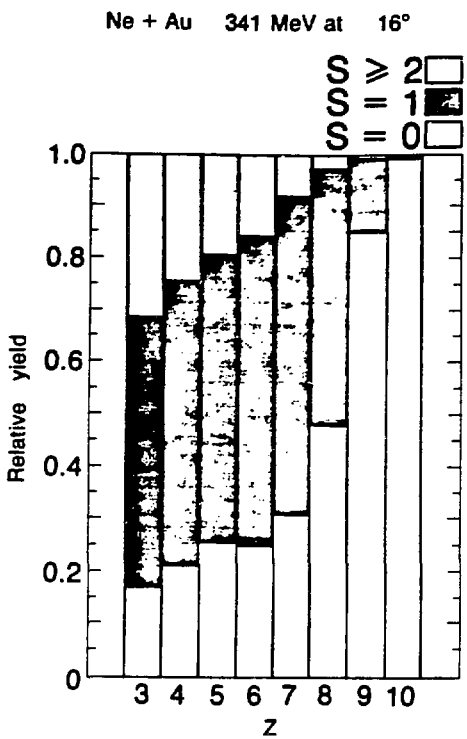

Fig. 5. The same as Fig. 4 for the bombarding energy of 341 MeV.

Ne. One obtains immediately from this figure an overview of the transfer/breakup relationship, and its dependence on the ejectile charge. The same information for the higher bombarding energy, 341 MeV, is shown in Fig. 5.

The next question is which wall or walls registered particles. The symmetry of the cube and location of the beam axis along a diagonal gives us forward/backward and in-plane/out-of-plane information. A crude form of angular correlation for the light particles is given in Fig. 6. For each PLF, the count rate in the different walls is indicated. Recall from Fig. 1 that walls 1 and 2 are in the forward direction, 3 and 4 are back of 90^{0} and walls 5 and 6 are up and down, respectively. In all cases, the forward walls are the most likely to observe a charged particle. The lighter PLF's (Li - C), however, are relatively more likely to be associated with particles in walls 3-6. It does not seem reasonable that these backward-going particles are the result of a projectile breakup reaction. The likely explanation is that they arise from the decay of the excited TLF by charged-particle evaporation. If this is indeed the case, these events belong in the category of a transfer reaction. The following consistency

Fig. 6 (right) The relative frequency with which each wall detects a light particle in coincidence with ejectiles from Li to F.

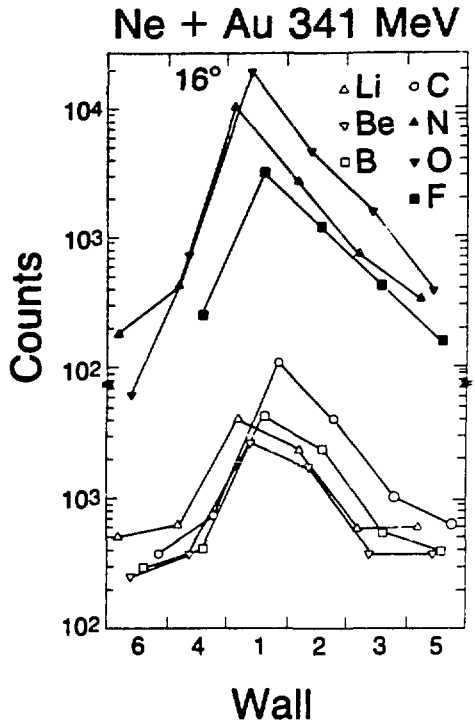

check was therefore made. Assuming a complete charge transfer occurred, the excitation energy and the angular momentum of the TLF were estimated for each PLF. These estimates were then used in a statistical model calculation[10] to calculate the competition among neutron, charged particle, and fission decay. These predictions were found to be consistent with the observations. In addition, the most likely form of charged particle decay was

Fig. 7. (below) The fraction of events that represent complete charge transfer for ejectiles at differenct angles. The shaded area gives the size of the correction for charged-particle evaporation by the target

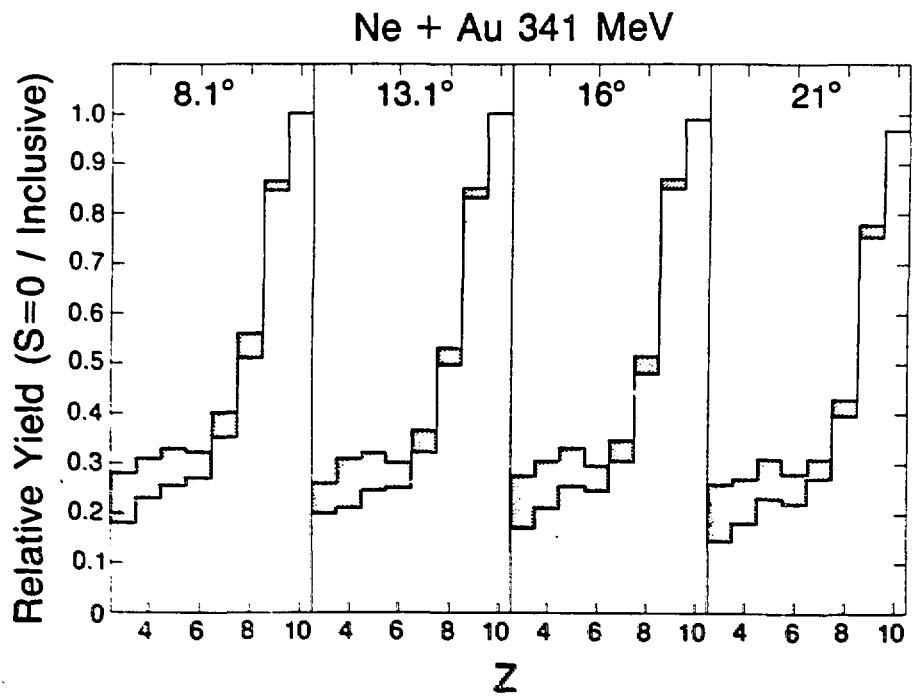

predicted to be proton (rather than alpha-particle) emission. A separate experiment done with improved particle identification was performed to check this prediction and it was verified. Given this consistency, a correction based on the particles detected by the backward walls was therefore applied to all walls in order to include these events in the classification of transfer events.

The dependence of the transfer/breakup relationship on the angle of the PLF is shown in Fig. 7. (The crosshatched area in each panel indicates the size of the evaporation correction described above. Henceforth, all references to transfer or "S = 0" events include this correction). This dependence varies slowly with angle and thus can be extrapolated with confidence. This enables us to use inclusive measurements at other angles to establish the differential cross sections for transfer and breakup over a range of angles wide enough to integrate and obtain total cross sections. Fig. 8 gives the inclusive angular distributions and the transfer component for oxygen, carbon, and lithium ejectiles. The interpolated and extrapolated values of the transfer differential cross sections are given by the dashed lines. The angle-integrated cross sections

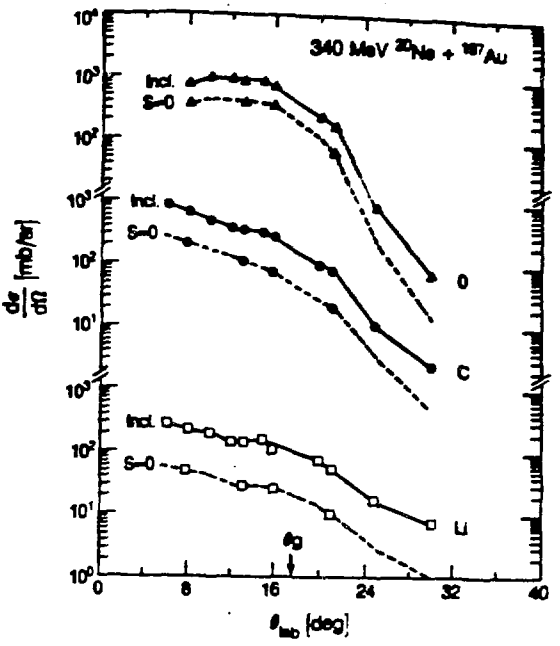

Fig. 8. Differential cross sections for inclusive and transfer reaction products.

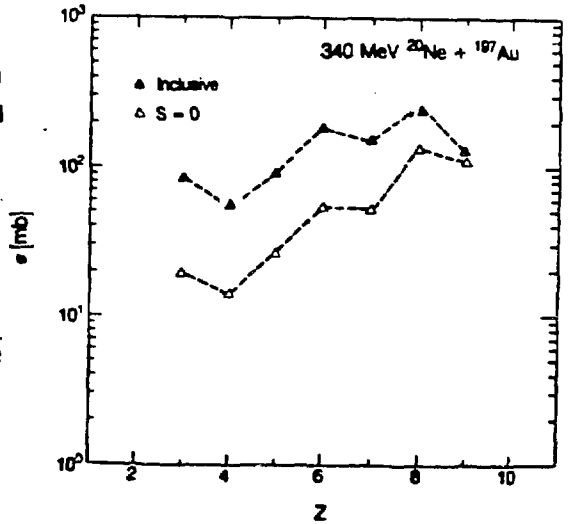

Fig. 9. Angle-integrated cross sections for inclusive and transfer reaction products.

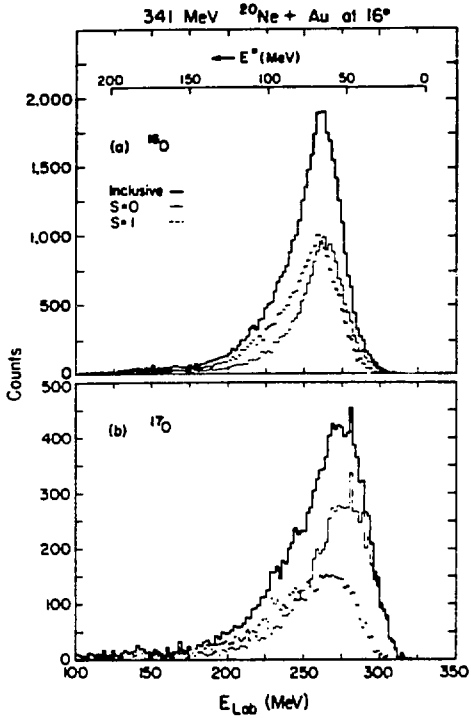

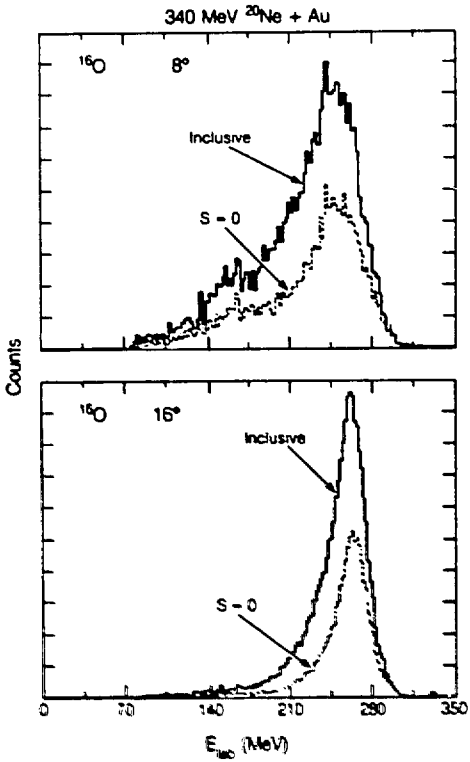

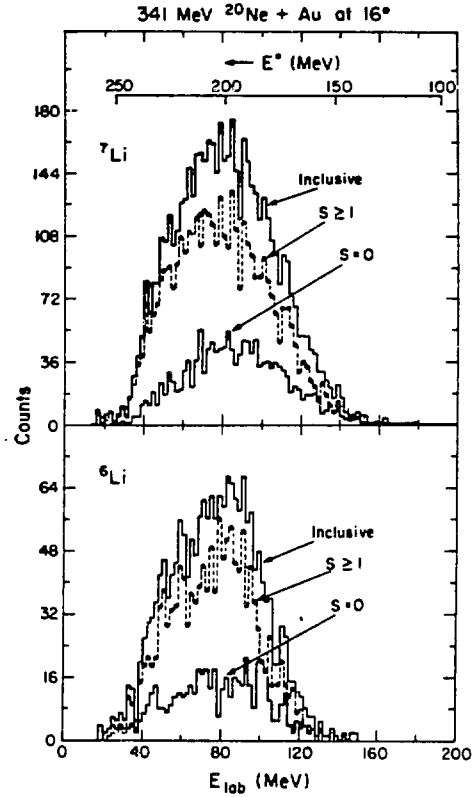

Fig. 10. (above left) Lab energy spectra of ^{16}O and ^{17}O ejectiles. The excitation energy E* is given for the reaction ^{197}Au(^{20}Ne,^{16}O) ^{201}Tl, which corresponds to S=0.

Fig. 11. (above right) Lab energy spectra of ^{7}Li and ^{6}Li ejectiles. The excitation energy E* is given for the reaction ^{197}Au(^{20}Ne,^{7}Li) ^{210}Rn, which corresponds to S=0.

Fig. 12. (left) Lab energy spectra of ^{16}O ejectiles at 16° and at 8°.

are presented in Fig. 9. The absolute errors are typically ±20%.

IV. B. Energy spectra.

One of the advantages of the plastic box over the streamer chamber is that it enables one not only to measure yields of various transfer reactions but also to acquire sufficient counting statistics to analyze energy spectra. The shapes of these spectra contain additional information on the reaction mechanism provided one is able to separate the contributing processes. The energy spectra for $^{16,17}O$ ions, produced by 341 MeV ^{20}Ne projectiles and observed at $\theta_{lab} = 16^{o}$, are shown in Fig. 10. While the inclusive spectra for ^{16}O and ^{17}O exhibit some differences (the ^{17}O spectrum is broader), the shape differences are more marked when the spectra are separated into their transfer and breakup components. The differences between the S = 0 and S = 1 spectra for ^{17}O are particularly evident. The characteristic shape of a spectrum also depends on whether the PLF is close to or far from the projectile mass. In Fig. 11, the spectra of $^{6,7}Li$ ejectiles are shown for the same scattering angle as in Fig. 10. The spectra in Fig. 11 are much more symmetric and closer in form to a Gaussian. A comparison of transfer reaction spectra at two different laboratory angles is shown in Fig. 12. In this case the spectrum shape changes considerably in going to angles forward of the grazing angle.

One way of obtaining a concise overview of the energy spectra for the many different PLF's is to examine the moments of the spectra rather than the spectra themselves.

The moments - mean value E, standard deviation σ, skewness γ_1, and kurtosis β_2, defined by

$$\bar{E} \equiv \langle E \rangle \equiv \frac{\int \frac{d\sigma}{dE} E\,dE}{\int \frac{d\sigma}{dE}\,dE}, \qquad \sigma \equiv (\langle E^2 \rangle - \bar{E}^2)^{1/2},$$

$$\gamma_1 \equiv \langle (E-\bar{E})^3 \rangle / \sigma^3, \qquad \beta_2 \equiv \langle (\bar{E}-E)^4 \rangle / \sigma^4,$$

have the advantage of an unambiguous, model-independent definition. In the case of the width, for example, use of the moment of the entire spectrum avoids the problem of choosing which portions of the spectrum to include or exclude when fitting a particular mathematical function to the spectrum. The moments are presented in Fig. 13 for the S = 0 and S = 1 components of the spectra for the most intense isotopes of each element. Each of the moments shows an overall trend as the charge and mass of the PLF vary. We shall come back to this in the discussion section.

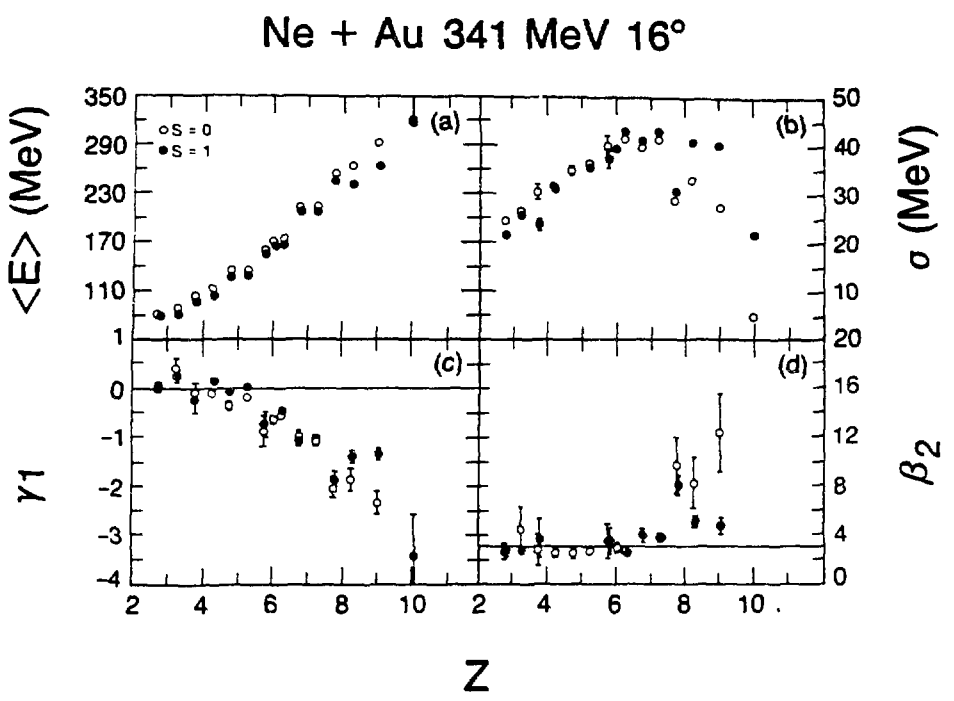

Fig. 13. The moments of the energy spectra. The PLF's are (left to right) $^{6,7}Li$, $^{7,9}Be$, $^{10,11}B$, $^{11,12,13}C$, $^{14,15}N$, $^{16,17}O$, ^{19}F, ^{20}Ne. Elastic scattering is excluded from the ^{20}Ne spectrum.

IV. C. Other information and limitations of the method.

In general, the multiplicity information from the plastic box for reactions at these energies may be fairly accurate even though the system is not highly segmented and even though there are only two walls covering the most forward angles. This is because the true multiplicities of reactions such as these (e.g., 16 MeV/u ^{16}O + CsI as measured by a streamer chamber[6]) are small, thus greatly reducing the probability of a multiple hit in a single wall.

Further information available from the plastic box consists of correlation patterns among the walls when two walls register particles. Since S = 2 events are at most 30% of the total for a given PLF, and generally much less, we will not discuss those results here.

It would be very desirable to know which type of particle was detected in a S = 1 event. The large solid angle of a given wall and the thickness of the first scintillator paddle severely restrict the particle identification capability of the system. It is only possible to say that the energetic particles observed in the forward paddles are mainly protons and alpha

particles. There does not seem to be much in the way of heavier fragments associated with any of the PLF's.

The light particles that are stopped in the cylindrical mounts holding the solid state telescopes are not recorded. Since the sequential decay process concentrates light particles in the general direction of the ejectile, the cross section for this effect amounts to a (maximum) 7% reduction to be made in the S = 0 cross sections.

The plastic box ignores not only neutrons evaporated by the target but also any neutrons associated with the projectile. An excited primary PLF may decay by neutron emission, of course. Thus, a detected ^{12}C might have originated as a ^{13}C, or an ^{16}O nucleus could be the product of an ^{17}O primary particle excited just above the neutron threshold. An examination of the separation energies for n, p, and α emission by nuclei from F to Li indicates that ^{17}O, $^{14,13}C$, and $^{10,9}Be$ are relevant cases in which the neutron threshold is below a threshold for charged particle emission. However, $^{9}Be^{*}$ decays to α + α + n and is thus removed from consideration. In order for a collision involving neutron emission from the ejectile to be <u>improperly</u> labeled as a transfer (S = 0) reaction, it must consist of neutron <u>without</u> any other emission of a fast charged particle (whether preequilibrium or sequential). The case in which this could occur and have an effect would be the feeding of ^{12}C by neutron emission from ^{13}C or ^{14}C. In other cases, e.g., ^{17}O, inclusive measurements[8] suggest the primary population of the neutron emitter to be small. The important point is that the plastic box does measure complete <u>charge</u> transfer without ambiguity, and this should have a strong correspondence in most cases to mass transfer.

V. Discussion.

It is useful to recall what the plastic box actually measures. A PLF observed without any associated charged particle is the result of a two-body reaction in which a transfer of nucleons to the target took place <u>and</u> the emerging PLF was produced in an excited state lying below the threshold for charged particle decay. This is a subset of a broader class of "transfer" reactions in which the light reaction partner (as well as the heavy partner)

may emerge in particle-unbound excited states that decay long after the collision is over. This subset, nevertheless, is a significant portion of the quasi-elastic cross section for Ne on Au at intermediate bombarding energies - even for very large mass transfers. This latter fraction is of the order of 1/2 at 11 MeV/u (Fig. 4) and is still about 1/3 at 17 MeV/u (Figs. 5 and 7). The first observation, therefore, is that this class of transfer reactions survives well into the intermediate energy region.

V. A. Reconstruction of primary cross sections.

A second observation is that the events having $S \geq 1$, the breakup reactions, are on the increase as the bombarding energy is increased. This behavior is expected and might be explained in at least two ways. One possibility is an increase in the preequilibrium emission of light particles from the region of contact between target and projectile. However, it is known that the sequential decay of heavy ions is a dominant mechanism in the production of beam velocity ejectiles in coincidence with forward going light particles.[5,11] In this case the determining factor in the decay of an ejectile is simply whether it is in an excited state above a particle decay threshold, i.e., it is the spectrum of excitation energy in the emerging fragment. (At high excitation energies the distinction between preequilibrium emission and sequential decay may blur.) It is a useful exercise to make the assumption that sequential decay is the dominant process and to see what information this permits us to gain from our measurements.

The assumption of sequential decay makes it possible to reconstruct the primary ejectile cross sections from the measured $S = 0$ and $S = 1$ cross sections. The information from the plastic scintillator walls suggests that mainly alpha particles or protons (as opposed to heavier charged particles) are in coincidence with the PLF. We will assume this to be the case. Thus, there are two possible charged-particle decay paths leading to the production of each observed ejectile and we will assume that the decay mode of each primary fragment is determined by its lowest threshold. In almost all cases,

the alpha threshold of a primary fragment is lower than the proton threshold. The energies of the first alpha-, proton-, and neutron-decaying states of the most prominent ejectiles are indicated in Fig. 14. Therefore, in most cases, the S = 1 events will be fed via alpha-decaying states (The assumption has been borne out by more recent coincidence experiments, which indicate a preponderance of alpha particles accompanying breakup.)

The low proton threshold of nitrogen provides an exception to this rule. As a result, the S = 1 carbon cross section could be expected to contain contributions from both oxygen and nitrogen breakup. Similarly, the S = 1 boron yield should be non-existent (sofar as our assumption that only the lowest thresholds contribute is valid). For these two cases, we have assumed that both proton and alpha sequential decays contribute to the observed breakup yield, and further assume that the relative contributions scale with the experimental S = 0 yields of the two possible primary nuclei. This provides us with a primary reconstruction as outlined schematically in Fig. 15.

The low-lying, neutron-decaying states of $^{14,13}C$ and ^{17}O have already been noted. While the presence of these states has an effect on the deduced breakup probabilities, they do not affect the accuracy of the reconstruction since the primary yields for a given Z will be summed over all isotopes.

The reconstruction procedure just outlined generates primary cross sections over the range of primary charge Z = 5-9. The primary lithium and beryllium yields cannot be estimated since the reconstruction procedure would require S = 1 alpha and proton cross sections that, if experimentally available, could come from a multitude of primary fragments.

The results of the experimental reconstruction of the primary ejectile charge yields are shown in Fig. 16, at both 11 and 17 MeV/nucleon. The cross sections for the production of the heaviest ejectiles are remarkably similar at both bombarding energies. The higher beam energy is seen to enhance the yields of massive charge-transfer products. Given our assumptions, it is apparent that the large cross sections observed for the production of light ejectiles at higher beam energies are due to two effects: increased excitation energy of the primary fragment as well as greater charge transfer prior to breakup.

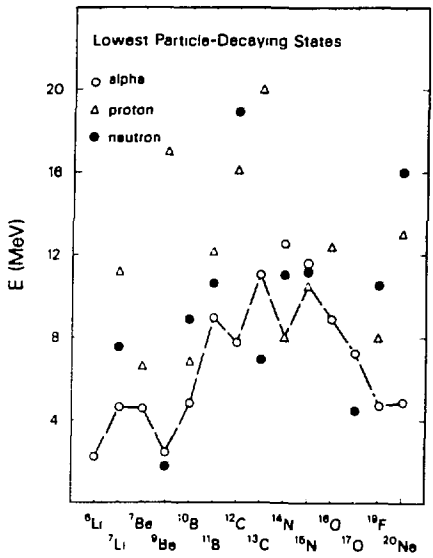

Fig. 14. The energy of the lowest alpha-, proton-, and neutron-decaying states for the most prominent ejectiles. The dashed line connects the lowest charged-particle decay thresholds.

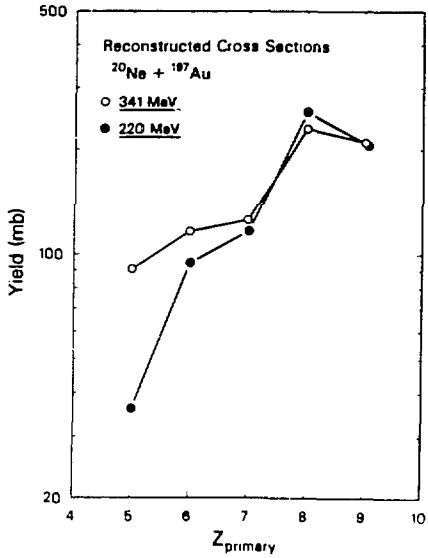

Fig. 16. The reconstructed primary cross sections plotted versus primary ejectile charge, as deduced from data at both bombarding energies.

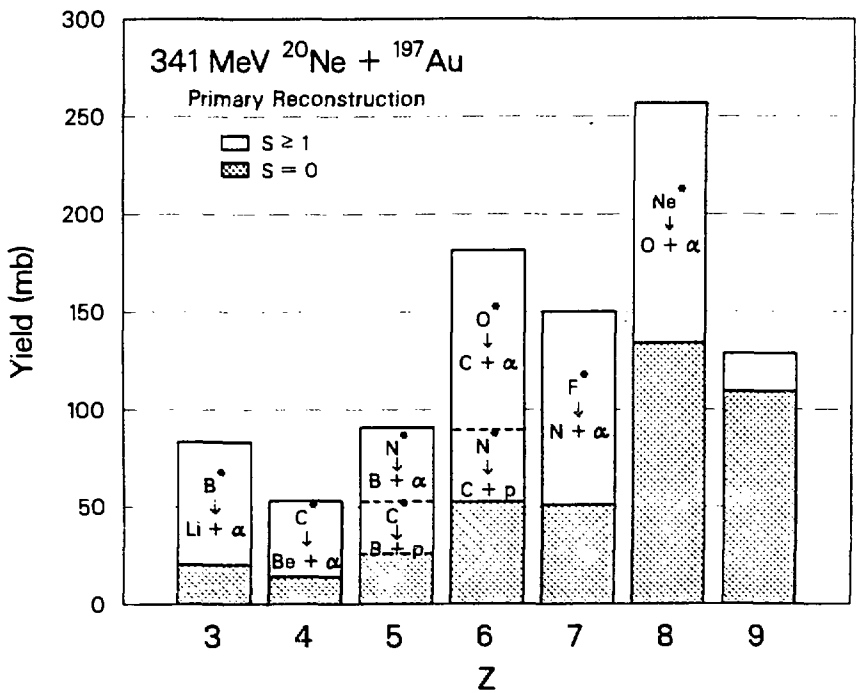

Fig. 15. The reconstruction of primary ejectiles for the results at 341 MeV.

The instability of ^{8}Be(g.s.) does not allow us to measure an S = 1 ^{8}Be cross section. Therefore, we miss a cross section that would have been added to the primary carbon yield in our reconstruction algorithm. For this reason, the reconstructed carbon yield will underestimate the abundance of primary carbon fragments.

V. B. Survival Fraction of the Primary Ejectiles, and the Division of Excitation Energy.

From the reconstructed primary cross sections we may calculate the probability that an ejectile will "survive" the transfer process without undergoing sequential decay. This is just the ratio of the S = 0 cross section to the total primary cross section and is of greater physical significance than the S = 0/inclusive ratio. The survival fractions calculated at 341 and 220 MeV are shown in Fig. 17.

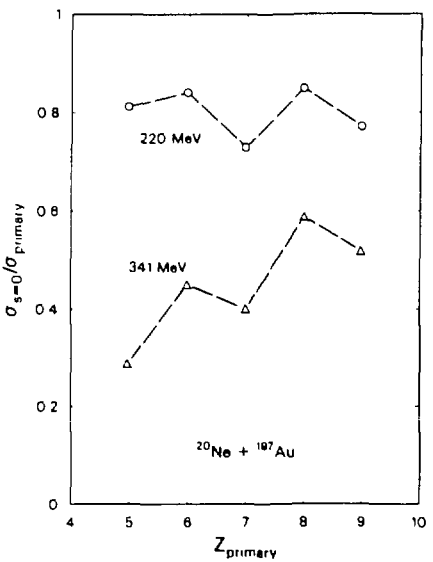

Fig. 17. The survival fractions are plotted as a function of primary ejectile charge at both bombarding energies. The larger values for carbon and oxygen may be associated with the unobserved removal of excitation energy by neutron decay of ^{14,15}C and ^{17}O primary fragments.

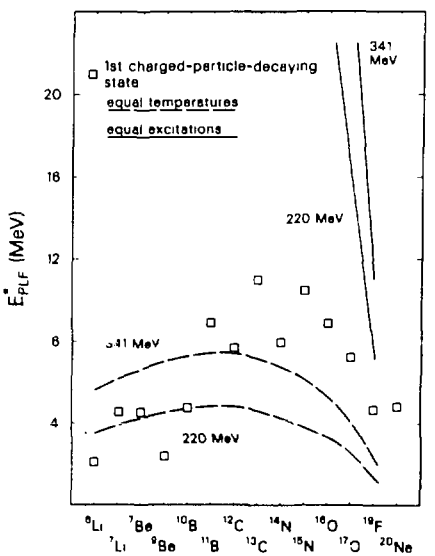

Fig. 18. The mean excitation energies of the primary fragments calculated under the extreme assumptions of equal excitation and division according to the masses. Also shown are the energies of the first charged- particle decaying states of the most prominent ejectiles.

As can be seen, the survival fractions are smaller at the higher bombarding energy. This can be understood in terms of the greater excitation associated with nucleon transfer at high energies. However, the striking aspect is that the survival fractions of the massive charge-transfer events are associated on the average with very large total excitation energies. This argues against an equal sharing of excitation energy between ejectile and target. However, if we assume that the excitation energy is divided unequally, for example as the ratio of the masses, then the values of the S = O/primary ratios can be understood at least qualitatively: while the more massive transfers to the target will result in greater excitation energies in the primary system, the correspondingly lighter projectile-like fragments will, in turn, have a smaller fraction of the total excitation.

This is illustrated in Fig. 18, where the first particle-decaying states of the various ejectiles are compared with the average excitation energies deposited in the primary ejectiles assuming either an equal-excitation or mass-proportional division of excitation energy. As can be seen, the latter, asymmetric division of excitation results in ejectile energies that track roughly with the decay thresholds. While such an analysis is not quanitative (lacking any information on the widths of the excitation-energy distributions), the observed survival fractions are more consistent with an excitation-energy division that is proportional to the mass asymmetry of the exit channel. We would like to note here that this asymmetric division of excitation energy does not necessarily imply that a high degree of equilibration has been reached in the collision. A direct transfer of several or many nucleons form light projectile to heavy target leaves the heavy partner with the responsibility of converting the transferred nucleons kinetic energy to excitation energy. The light partner need only have the transferred nucleons removed, and the energies associated with this are less than 11 or 17 MeV per nucleon.

V.C. Energy spectra.

Consider next the shapes of the energy spectra. The mean energies, shown for both S = 0 and S = 1 reactions in Fig. 13a, are remarkably regular. They increase approximately linearly with the mass of the ejectile, as expected for PLF's with a beam-like velocity. The mean value for a two-body reaction is always higher than for a three-body reaction. This may be simply understood in terms of the additional excitation energy required to separate the third body. Note that for the isotopes of nitrogen and lighter PLF's, the trends in the mean energies for S = 0 and S = 1 are identical.

The standard deviations or widths of the spectra show a behavior with fragment mass that is (very roughly) reminiscent of the parabolic dependence found in high energy fragmentation.[12] Indeed, conversion of the energy widths for transfer or breakup to reduced momentum widths, σ_0, as in Ref. 12, yields a range of values (see Fig. 19) that fits into the existing systematics.[13] Referring again to Fig. 13b, relatively large differences between S = 0 and S = 1 widths are found for ^{7}Be, ^{17}O, and ^{19}F. For isotopes of nitrogen and lighter PLF's, the trends exhibited by the S = 0 and S = 1 widths are very similar. As the PLF becomes further removed from the projectile, the shape of the spectrum becomes more symmetric and Gaussian-like, i.e., $\gamma_1 \to 0$ and $\beta_2 \to 3$. Again, for $Z \leq 7$, the behavior of γ_1 and β_2 are identical for S = 0 and S = 1.

The above observations on the moments of the spectra suggest that the transfer of three or more charge units is a natural dividing line. Smaller transfers, e.g., an alpha particle or less, are associated with spectra that may change rapidly in shape. The spectra for larger mass transfers change

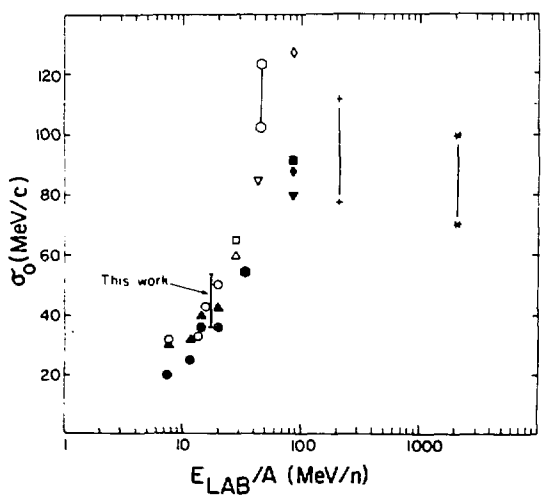

Fig. 19. The systematics of reduced momentum widths for PLF's from many reactions vs. lab energy. For references see Ref. 13.

more slowly and regularly from one isotope and element to the next (Note in Figs. 10 and 11 the similarity of the ^{6,7}Li spectra and the differences for ^{16,17}O.) This dividing line is also reflected in the ratio of transfer to inclusive yields (Figs. 5 and 7). The qualitative conclusion to draw from this is that the transfer of an alpha particle or less occurs in a very short time, i.e., is a fast "direct" reaction, whereas larger transfers are more characteristic of the fusion process. The fusion of heavy projectiles with heavy targets exhibits cross sections that vary smoothly with projectile mass provided one is well above the barrier, as is the case here. Few-nucleon transfer reactions, however, exhibit spectra that may change rapidly as the number of captured nucleons increases.

V. D. Comparison with Models.

The qualitative remarks above could be sharpened or tested by quantitative comparisons with the predictions of different models provided the model and the experiment predict and measure the same quantity. As we shall see, the comparisons possible at present are few. Consider first the angle-integrated cross sections. The sum rule model of Wilczynska, et. al.,[14] for incomplete fusion would be a natural starting point, and indeed it is straightforward to make a calculation based on the parameters of Ref. 14. As may be seen in Fig. 20 the agreement with the present experiment is poor.

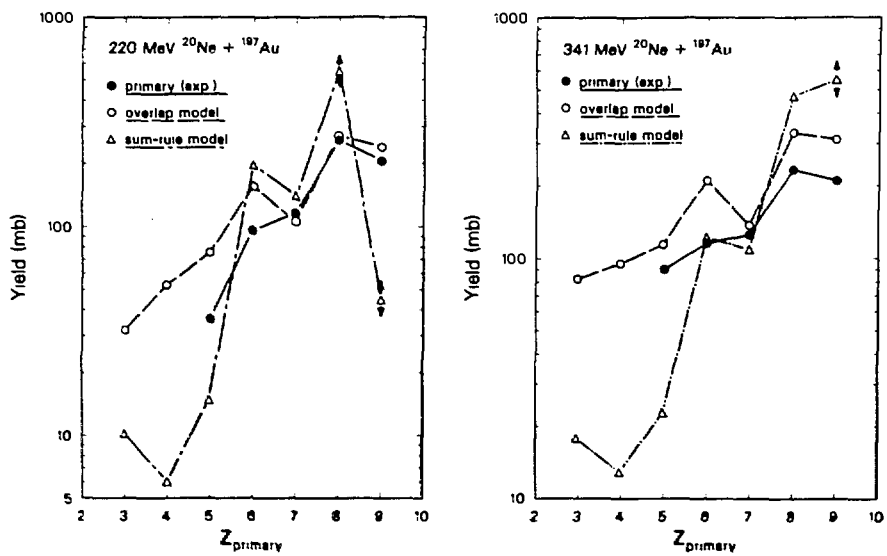

Fig. 20 The predictions of the sum-rule and overlap models are compared with reconstructed primary cross sections at 220 MeV and 341 MeV.

The overlap model[15] of Harvey and Homeyer calculates the yield of PLF's by assuming that the projectile can be factored into two portions, according to the fragmentation model of Friedman,[16] and that there must be a geometrical overlap of the portion to be removed and the target. The calculation reproduces the main trends in the experimental results.

The shapes of the spectra clearly provide an important point of comparison. Some of the early theoretical effort in this area was by McVoy and Nemes,[17] who calculated energy spectra in a plane-wave approximation for both transfer and breakup. A general consequence of their assumptions is that the momentum-, and hence energy-width for breakup should always exceed that for transfer. This prediction is borne out by the experiment for PLF's at the grazing angle with Z very close to that of the projectile. However, the reverse is true at a more forward angle, $\theta_{lab} = 8^{o}$. Here, the widths for transfer are (with the one exception of ^{19}F) all larger than those for breakup! The complexity of the energy widths is illustrated by the interesting change in the ^{16}O spectra in going from the grazing angle to the forward angle of 8^{o} (see Fig. 12). The 8^{o} spectrum is highly skewed - perhaps the more pronounced low energy tail reflects scattering from the far side of the target nucleus.

Other more elaborate models for which these energy spectra present an excellent opportunity for analysis are the direct-reaction models - the DWBA for the transfer of smaller masses,[18] and a multistep extension of the DWBA, the breakup-fusion model, for the larger mass transfers.[19] The S = 0 spectra are well suited for comparison with a DWBA calculation because one knows that the spectra are uncontaminated by breakup and that the excited states of the projectile that must be included in the calculation are limited to a relatively few bound states. The DWBA based on the diffraction model and extensively applied by Mermaz, et. al.,[18] would seem well suited for the analysis of the present data for $Z \geq 8$.

Models appropriate for more massive transfer reactions are based on a two-step process: the projectile is separated into two parts, one of which then fuses with the target. The overlap model[15] is an example involving geometrical overlap for the second step. A more sophisticated approach is

the breakup-fusion model developed by Udagawa, et. al., which incorporates distorted waves.[19] This model has been applied to a few cases at lower bombarding energies, e.g., at 6.8 MeV/u $^{14}N + ^{159}Tb$ for alpha-particle ejectiles.[19] It would be of interest to see how well it does in describing a reaction at higher energies covering a wide range of PLF's.

VI. Summary and Outlook.

Transfer and breakup reactions have been identified in the collisions of 11 and 17 MeV/u ^{20}Ne with Au. A 4π plastic scintillator system was used to separate the two types of reactions by detecting the presence or absence of additional light charged particles associated with the PLF. Angular distributions, total cross sections, and energy spectra were measured. The properties of the quasi-elastic reaction products are similar and vary smoothly for both transfer and breakup for PLF's with Z = 3 to 7, whereas for heavier ejectiles the behavior is less systematic. The assumption of sequential decay permits a reconstruction of the primary cross sections. A comparison of the absolute cross sections with the overlap model[15] yields favorable results. The significant probabilities for producing an ejectile in a particle-bound state suggests that, on the average, most of the excitation energy is deposited in the heavy fragment, at least for the case of mass transferred from a light projectile to a heavy target.

At present, it appears that the charged particles accompanying a PLF are mainly protons and alpha particles rather than heavier ions. In the future it will be possible to identify the light particles and measure their angles with position-sensitive plastic walls that have been developed.[20] Such experiments should enable a more precise reconstruction of the primary yields and excitations from the observed sequential decay products.

References

1) M. Buenerd et al., Phys. Rev. Lett. 37, 1191 (1976).
2) T. Inamura et al., Phys. Lett. 69B, 51 (1977).
3) H. W. Wiltschut et al., Phys. Lett. 123B, 173 (1983).
4) U. Jahnke et al., Phys. Rev. Lett. 50, 1246 (1983).
5) W. Rae et al., Phys. Lett. 105B, 417 (1981).
6) M. J. Murphy et al., Phys Lett. 120B, 319 (1983).
7) K. Van Bibber et al., IEEE Trans. Nucl. Sci. NS-31 35 (1984)
8) Ch. Egelhaaf et al., Nucl. Phys. A405, 397 (1983).
9) B. G. Harvey and M. J. Murphy, Phys. Lett. 130B, 373 (1983).
10) M. Blann, private communication.
11) H. Homeyer, et al., Phys. Rev. C26 1335 (1982).
12) A. S. Goldhaber, Phys. Lett. 53B 306 (1974).
13) M. J. Murphy and R. G. Stokstad, Phys. Rev. C28, 428 (1983).
R. G. Stokstad, Comm. on Nucl and Part. Phys. (1984).
14) J. Wilczynski et al., Nucl. Phys. A373, 109 (1982).
15) B. Harvey and H. Homeyer, LBL preprint 16882 (1983).
16) W. Friedman, Phys. Rev. C27, 569 (1983).
17) K. W. McVoy and M. C. Nemes, Z. Physik A295, 177 (1980).
18) M. C. Mermaz, Phys. Rev. C21, 2356 (1980), C28, 1587 (1983).
19) T. Udagawa, Proc. Int. Conf. Bad Honnef (1984); Phys. Lett. 135B, 333 (1984).
20) M. Bantel et al., Nucl. Inst. Meth. 226, 394 (1984).